Terahertz electro-optic wavelength conversion in GaAs quantum wells: Improved efficiency and room-temperature operation

S. G. Carter,[a] V. Ciulin, and M. S. Sherwin
Department of Physics and iQUEST, University of California, Santa Barbara, California 93106

M. Hanson, A. Huntington, L. A. Coldren, and A. C. Gossard
Materials Department, University of California, Santa Barbara, California 93106

(Received 3 July 2003; accepted 8 December 2003)

A 4-μm-thick sample containing 50 GaAs/AlGaAs asymmetric coupled quantum wells was driven with a strong terahertz (THz) electric field of frequency ω_{THz} and probed with a near-infrared (NIR) laser of frequency ω_{NIR}. The THz beam modulated the probe to generate sidebands at $\omega_{\mathrm{NIR}} + n\omega_{\mathrm{THz}}$, where n is an integer. Up to 0.2% of the NIR laser power was converted into the $n=+1$ sideband at 20 K, and sidebands were observed up to room temperature. The strong THz fields also induced changes in the NIR absorption of the sample. © *2004 American Institute of Physics.* [DOI: 10.1063/1.1645662]

In an efficient wavelength division multiplexed (WDM) optical communication network, it is necessary to switch data from one near-infrared (NIR) wavelength to another.[1] Wavelength conversion has been performed all-optically in semiconductor optical amplifiers,[1,2] semiconductor lasers,[3] optical fibers,[4] $LiNbO_3$,[5] and in bulk GaAs.[6] In previous work, we have demonstrated all-optical wavelength conversion by THz electro-optic (EO) modulation in GaAs quantum wells.[7–12] This method is not limited in speed by gain and carrier dynamics, as are SOAs and lasers, and has the advantage of occurring in a system with strong nonlinearities[13] and resonances that can be tuned by electric fields[7] and band-gap engineering.

The THz EO modulation involves a NIR beam of frequency ω_{NIR} that mixes with a THz beam of frequency ω_{THz} in a GaAs/AlGaAs heterostructure. Sidebands are emitted at $\omega_{\mathrm{sideband}}=\omega_{\mathrm{NIR}}+n\omega_{\mathrm{THz}}$, where $n=\pm 1,2,3$, etc. For low THz fields the resonant structure of sideband conversion can be well described by a resonant nonlinear susceptibility model, in which sidebands are strongest when ω_{NIR} is resonant with interband transitions and ω_{THz} is resonant with intersubband transitions.[9] The resonances can be modified by changing the sample structure or by applying a dc voltage.[7] For stronger THz fields, the sideband resonances change as the THz field "dresses" the exciton states.[12,14]

This letter reports sideband conversion efficiencies more than 10 times higher than the best previous results using THz EO modulation.[7] Sidebands are also observed at room temperature. Finally, the strong THz field influences the exciton states and the resonant structure of the sideband generation. The key to the improvements over previous work is sample design. The sample studied here has a much larger interaction length, and it was designed to transmit the NIR beam and sidebands instead of reflecting them from a distributed Bragg reflector (DBR). Since the frequencies of excitonic resonances shift strongly with temperature, the elimination of the fixed-bandwidth DBR greatly simplified the measurement of sidebands for a wide range of temperatures (20–295 K).

The sample consists of 50 periods of double GaAs quantum wells, nominally 100 and 120 Å wide and separated by a 25 Å $Al_{0.2}Ga_{0.8}As$ tunnel barrier (see inset of Fig. 1). Each pair of wells is separated by a 200 Å $Al_{0.3}Ga_{0.7}As$ barrier. The difference between the widths of the GaAs wells breaks inversion symmetry in the growth direction, thus allowing the generation of sidebands with odd n.[8] Furthermore, the tunnel splitting produces a spacing between electron subbands in the range of our THz source,[7] the UCSB Free Electron Laser. The semi-insulating GaAs substrate absorbs NIR radiation resonant with excitonic transitions. In previous experiments on similar coupled quantum wells, NIR and side-

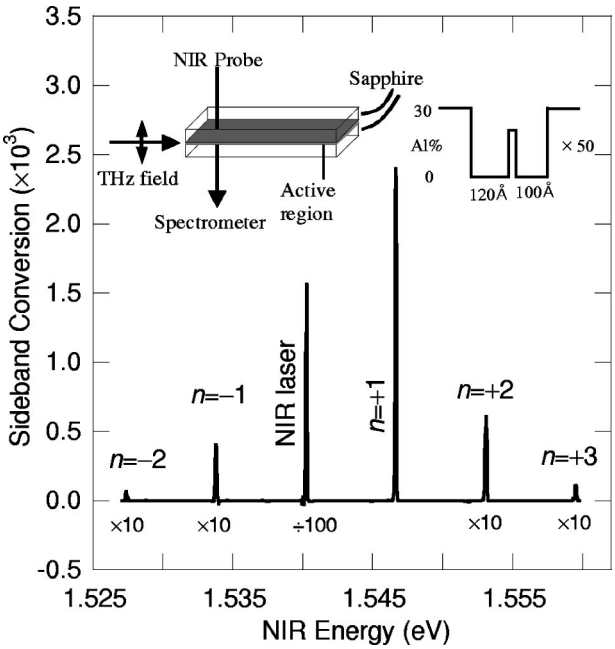

FIG. 1. Transmitted sideband spectrum taken at 20 K with a FEL frequency of 1.5 THz (6.4 meV). The transmitted beam at ω_{NIR} is divided by 100 and the $n=+3$, $+2$, -1, -2 sidebands are multiplied by 10 for clarity. The THz power was ~1 kW and the NIR power was 0.2 mW. The experimental geometry and the conduction band diagram of a sample well are inset in the figure.

[a]Electronic mail: scarter@physics.ucsb.edu

bands have been reflected off a DBR placed between the QW and the substrate. To allow transmission of the NIR probe through the present sample, the sample was glued to a piece of sapphire and the semi-insulating GaAs substrate was etched away. This left a 4-μm-thick epitaxial layer glued to sapphire, which included a 2.2-μm-active region, 0.7 μm of buffer layers, two doped gate QWs (unused), and a 1-μm-etch stop layer. The sample was then glued to another piece of sapphire so that the active region was in the middle of a dielectric waveguide, maximizing the THz field.

The experimental geometry is shown in the inset of Fig. 1. The sample was placed in a closed-cycle He cryostat, where its temperature could be varied from room temperature down to 18 K. The THz beam was coupled into the edge of the sample with its polarization perpendicular to the plane of the QW. The THz beam was on for about 4 μs at a repetition rate of 1.5 Hz with a peak power of $\sim$1 kW. It was focused onto the sample with an off-axis parabolic mirror ($f/4$) to a spot measured to be about 1.2 mm in diameter, yielding a maximum intensity of $\sim$90 kW/cm^2 ($\sim$2 kV/cm in the sample).

The NIR beam came from a cw tunable Ti:sapphire laser which was chopped by an acousto-optic modulator into $\sim$200 μs pulses that overlapped each THz pulse. The beam was incident perpendicular to the sample and typically focused to an intensity of roughly 5 W/cm^2, yielding an exciton density of about 10^9 cm^{-2} when tuned in resonance with the exciton transition. It then passed through the sample and was sent to a 0.85 m double monochromator, where it was detected by a photomultiplier tube (PMT). For measurements of the change in transmission by the THz field, the transmitted laser beam was sent directly to a silicon photodiode.

Figure 1 shows a typical sideband spectrum. The transmitted laser line at 1.54 eV (attenuated by 100) had sidebands at multiples of 6.4 meV (1.5 THz), the THz frequency. The $n=+1$ sideband was far stronger than the others with an intensity of about 0.2% of the incident NIR beam. This sideband spectrum was measured with an incident NIR intensity of about 2.5 W/cm^2, so the sideband intensity was about 5 mW/cm^2. For higher incident intensity of about 40 W/cm^2, the sideband intensity saturated near 25 mW/cm^2. The conversion efficiency of 0.2% was an order of magnitude higher than in previous work.[7] The increase is attributed to the five-fold increase in the interaction length of the sample, which is still only 2 μm.

The THz EO effect that gives rise to sidebands in our sample is different from the conventional EO effect in that both the THz and NIR frequencies are close to resonances of the sample. This resonant structure is shown in a sideband resonance spectrum in Fig. 2(b), taken by changing the incident NIR frequency while always moving the spectrometer to measure the $n=+1$ sideband. Figure 2(a) displays the exciton absorption lines in the transmission spectra for comparison. The lines have been assigned by comparison with theory.[15] The exciton formed by an electron in the nth conduction subband and a hole in the mth heavy hole subband is called EnHHm. The strongest sideband resonance at 1.533 eV (which appears to be split for lower THz power) had the incident NIR frequency resonant with E1HH2 and the 1.3 THz frequency (5.5 meV) resonant with the E1HH2–E2HH1

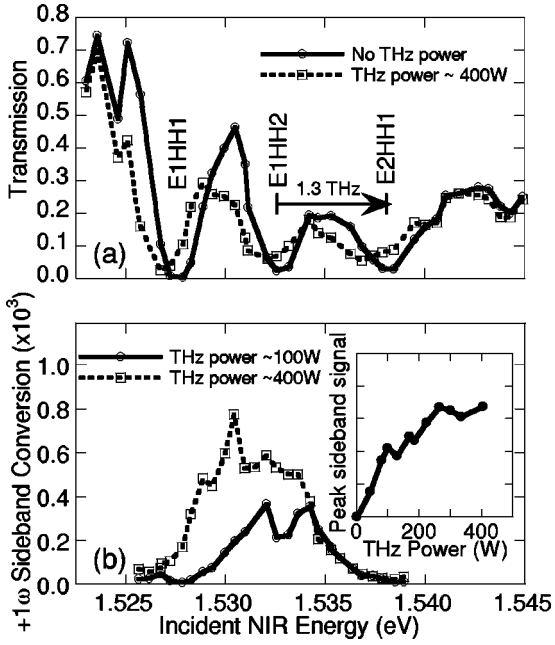

FIG. 2. (a) Sample transmission spectrum at 20 K taken when the FEL is off (open dots and solid lines) and at high power (open squares and dashed lines), indicating the effect of the strong THz field on the linear absorption. The absorption lines are labeled by theory (see Ref. 15). The arrow illustrates that the THz field is close to resonance with the E1HH2–E2HH1 transition. (b) Two $n=+1$ sideband resonance spectra at 20 K taken at low THz power (open dots and solid lines) and high THz power (open squares and dashed lines), indicating the change in resonant structure at high THz powers. Each point of the resonance spectra represents the $n=+1$ sideband signal when the NIR laser frequency is tuned to the value on the horizontal axis. The inset shows the $n=+1$ sideband peak intensity dependence on THz power. For each graph the FEL was at 1.3 THz (5.5 meV).

transition, a double resonance. (A more detailed discussion of this resonance can be found in Ref. 7.) The splitting was actually due to the strong absorption of both the incident NIR beam and the sideband when on resonance. This was confirmed by a coupled amplitude equation model[16] that propagated the sideband and incident laser through the sample as a function of wavelength and thickness. The model includes the nonlinear susceptibility and absorption loss. The significant increase in sideband conversion compared to samples 5 times shorter is consistent with this model.

Changes in the absorption, due to the strong THz field, modified the sideband resonances. Figure 2(a) displays the NIR transmission with and without a strong THz field. The excitonic absorption features redshifted, broadened, and absorbed less strongly when the THz field was on. The effects decreased as the THz field decreased but were qualitatively similar. Driving with 1.5 THz produced similar results as well. These changes were also manifest in the sideband resonance spectra shown in Fig. 2(b). The resonance spectrum at high THz field was redshifted, broadened, and the dip due to absorption was essentially gone. This could be due to the peak broadening and the decrease in absorption when the THz field was on. The inset graph shows the peak sideband signal as a function of THz power, illustrating the saturation that occurred at high powers. Some of these effects were directly due to strong THz fields.[12,14] However, some changes in the transmission persisted after the FEL pulse was turned off, indicating that the sample was heated during the FEL pulse. The heating effects could not be separated from

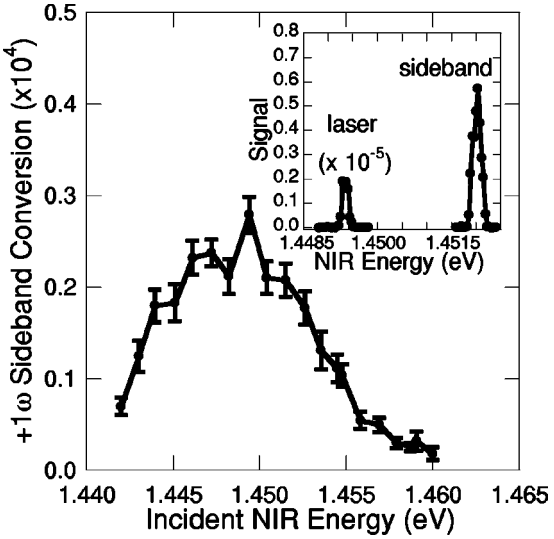

FIG. 3. Transmitted sideband spectrum (inset) and the $n=+1$ sideband resonance spectrum taken at 295 K with FEL frequency 0.66 THz (2.7 meV). Each point of the resonance spectrum represents the $n=+1$ sideband signal when the NIR laser frequency is tuned to the value on the horizontal axis. The THz power was ~6 kW and the NIR power was 3.2 mW.

the strong field effects, making a detailed understanding of changes in transmission impossible. The persistent heating effect did not come from photogenerated carrier heating as the effect has very little dependence on NIR power. Heating of carriers from residual extrinsic doping, or of the GaAs or sapphire lattice directly by the THz field could be the cause. This persistent effect was strong in samples with substrates removed, like the one studied here. A sample from the same wafer but with its substrate still attached exhibited changes in reflectivity during FEL pulses with very little persistent change, strongly supporting our conclusion that the changes in transmission reported here were not wholly due to heating. Further work in samples that do not exhibit persistent heating is being performed.

Sidebands were also generated at room temperature, as shown in Fig. 3. The figure displays the $n=+1$ sideband spectrum inset in a sideband resonance spectrum. At this temperature both the band gap and the intersubband spacing decreased, so ω_{THz} was reduced to 0.66 THz (2.7 meV). The fraction of the incident NIR beam converted to the sideband was about 3×10^{-5}, much smaller than at 20 K. A series of measurements were performed on the temperature dependence of the sideband generation. Thermal cycling produced irreversible changes in the optical spectra that were likely due to strain in the thinned sample. Thus the results varied from one cooldown to the next. However, compared to 20 K, the sideband conversion of this sample decreased by not more than a factor of 3 at 100 K and by not more than a factor of 10 at 200 K. The decrease in conversion came from at least two factors. First, the exciton linewidths broadened with increasing temperature, which decreased the peak nonlinear susceptibility and indicated an increase in the dephasing rate. This is demonstrated by how broad the sideband resonance spectrum is in Fig. 3 compared to Fig. 2(b). Second, while the sapphire is transparent to THz frequencies at low temperatures, it is absorbing ($\alpha\sim3\,\mathrm{cm}^{-1}$) at high temperatures.[17] This could have significantly decreased the THz field in the sample.

In summary, we performed terahertz EO experiments in a GaAs multi-quantum well sample that generated sidebands with an efficiency up to 0.2%. The sample also exhibited an interesting change in absorption that was partially due to strong THz field effects. The sideband conversion efficiency is not close to any fundamental limits of which we are aware, but is sufficient to be regenerated to full power by optical amplifiers. It is also comparable to efficiencies achieved in wavelength converters based on SOAs[2] or semiconductor lasers.[3] By comparison, a 4-μm-thick $LiNbO_3$ sample in the same experimental conditions should have a conversion efficiency of $\sim3\times10^{-8}$, assuming an EO coefficient of 9.6 pm/V.[18] Our device operated from 20 K up to room temperature, but had significantly decreased conversion efficiency at higher temperatures. This could be overcome by coupling the NIR light into the quantum well plane, further increasing the interaction length. A device like the one measured could be made voltage tunable as in Refs. 7 and 12 and could be implemented in InGaAs wells on InP for operation at 1.55 μm. The extremely small thickness of our wavelength converter makes it suitable for insertion into microphotonic circuits. Recently developed THz quantum cascade lasers[19] have, inside their cavities, THz electric fields comparable to the ~kV/cm fields used in this study.[20] Thus, all-semiconductor THz EO wavelength converters with integrated THz sources may be achieved in the future.

The authors thank David Citrin and Alex Maslov for helpful discussions. This research was funded by NSF-DMR 0070083 and SUN Microsystems. V.C. thanks the Swiss NSF for additional support.

[1] D. Nesset, T. Kelly, and D. Marcenac, IEEE Commun. Mag. **36**, 56 (1998).
[2] M. L. Masanovic, V. Lal, J. S. Barton, E. J. Skogen, D. J. Blumenthal, and L. A. Coldren, IEEE Photonics Technol. Lett. **15**, 1117 (2003).
[3] A. Hsu and S. L. Chuang, IEEE Photonics Technol. Lett. **15**, 1120 (2003).
[4] K. Torri and S. Yamashita, J. Lightwave Technol. **21**, 1039 (2003).
[5] M. Asobe, O. Tadanaga, H. Miyazawa, Y. Nishida, and H. Suzuki, Opt. Lett. **28**, 558 (2003).
[6] M. A. Zudov, J. Kono, A. P. Mitchell, and A. H. Chin, Phys. Rev. B **64**, 121204 (2001).
[7] M. Y. Su, S. G. Carter, M. S. Sherwin, A. Huntington, and L. A. Coldren, Appl. Phys. Lett. **81**, 1564 (2002).
[8] C. Phillips, M. Y. Su, M. S. Sherwin, J. Ko, and L. Coldren, Appl. Phys. Lett. **75**, 2728 (1999).
[9] M. Y. Su, C. Phillips, J. Ko, L. Coldren, and M. S. Sherwin, Physica B **272**, 438 (1999).
[10] J. Kono, M. Y. Su, T. Inoshita, T. Noda, M. S. Sherwin, S. J. Allen, and H. Sakaki, Phys. Rev. Lett. **79**, 1758 (1997).
[11] J. Cerne, J. Kono, T. Inoshita, M. Sherwin, M. Sundaram, and A. C. Gossard, Appl. Phys. Lett. **70**, 3543 (1997).
[12] M. Y. Su, S. G. Carter, M. S. Sherwin, A. Huntington, and L. A. Coldren, Phys. Rev. B **67**, 125307 (2003).
[13] F. Capasso, C. Sirtori, and A. Y. Cho, IEEE J. Quantum Electron. **30**, 1313 (1994).
[14] A. V. Maslov and D. S. Citrin, Phys. Rev. B **62**, 16686 (2000).
[15] M. Y. Su, Ph.D. thesis, University of California, Santa Barbara, 2002.
[16] R. W. Boyd, *Nonlinear Optics* (Academic, San Diego, 1992), Chap. 2, p. 69.
[17] E. V. Loewenstein, D. R. Smith, and R. L. Morgan, Appl. Opt. **12**, 398 (1973).
[18] R. W. Boyd, *Nonlinear Optics* (Academic, San Diego, 1992), Chap. 10, p. 404.
[19] R. Kohler, A. Tredicucci, F. Beltram, H. E. Beere, E. H. Linfield, A. G. Davies, D. A. Ritchie, R. C. Iotti, and F. Rossi, Nature (London) **417**, 156 (2002).
[20] D. S. Citrin (private communication).